Available online at www.sciencedirect.com

ScienceDirect

Procedia CIRP 82 (2019) 438–443

www.elsevier.com/locate/procedia

17th CIRP Conference on Modelling of Machining Operations

Thermomechanically coupled numerical simulation of cryogenic orthogonal cutting

Benedict Stampfer[a,*], Philipp Golda[b], Frederik Zanger[a], Robert Schießl[b], Ulrich Maas[b] and Volker Schulze[a]

[a]*wbk Institute of Production Science, Karlsruhe Institute of Technology (KIT), Kaiserstr. 12, 76131 Karlsruhe, Germany*
[b]*Instiute of Technical Thermodynamics (ITT), Karlsruhe Institute of Technology (KIT), Kaiserstr. 12, 76131 Karlsruhe, Germany*

* Corresponding author. Tel.: +49-721-608-42455; fax: +49-721-608-45004. *E-mail address:* benedict.stampfer@kit.edu

Abstract

During machining of Ti-6Al-4V, high thermal loads arise, which demand for advanced cooling concepts, such as the application of liquid nitrogen. An efficient approach to analyze the thermomechanical mechanisms which influence the tool life and the workpiece distortions is the usage of coupled numerical simulations.
In this work, the Finite-Element-Method was used to simulate the tool-workpiece-interaction and the chip formation, whereas the detailed treatment of the nitrogen fluid flow and its heat transfer is solved by an in-house program using the Finite-Difference-Method. Both simulations are coupled by appropriate boundary conditions, which are updated iteratively during the calculation.

Peer-review under responsibility of the scientific committee of The 17th CIRP Conference on Modelling of Machining Operations

Keywords: Cryogenic machining; Thermal analysis; Coupled simulation

1. Introduction

The alloy Ti-6Al-4V regarded in this work, is a common material for lightweight applications due to its good specific strength. However, the material's properties of high ductility, strength and low thermal conductivity cause high thermal loads and severe tool wear during machining. For such hard to machine materials, process cooling is crucial. In this work liquid nitrogen (LN_2) is used as cooling medium. LN_2 is non-toxic, environmentally harmless and has a large cooling potential. The absence of cutting emulsion and prevention of oxidation by LN_2 also results in an easier chip recycling. In this work, different variants of LN_2 application are regarded, namely rake face cooling and tool internal cooling. Numerical simulations are used here to design and adjust each variant, as well as to evaluate its effectiveness and efficiency. The simulation consists of a heat transfer model and a finite element chip formation simulation. Both models are coupled by boundary conditions depending on the cooling application.

2. State of the art

LN_2 assisted machining has been investigated by many researchers over the last 20 years. Among others the interaction between the heat transfer of the cutting tool, the workpiece material and the cooling medium LN_2 is of scientific interest.

2.1. Heat transfer in LN_2 cooling

Cryogenic media, e.g. LN2, are widely used in a variety of machining applications to generate a well-defined heat flux from the workpiece and the tool [1, 2].

Liquid nitrogen is particularly effective as a cryogenic cooling liquid, since on the one hand the high temperature differences between the object to be cooled and the fluid lead

2212-8271
Peer-review under responsibility of the scientific committee of The 17th CIRP Conference on Modelling of Machining Operations
10.1016/j.procir.2019.04.036

to large temperature gradients and thus to a correspondingly high cooling effect [3]. On the other hand, the energy, which is extracted from the solid to the liquid is used to overcome the evaporation enthalpy [3], resulting in an evaporation flux without any further increase of the fluid's temperature [3].

However, to enable the modeling of such cryogenic cooling processes it is necessary not only to consider the liquid phase, but also the gas phase and the evaporation process. Furthermore, the flow-regime of the two-phase impacts the resulting heat transfer in a massive way [3].

The physical properties of nitrogen change significantly during the evaporation process and the associated phase transition [4]. While the specific heat capacity is only reduced by a factor of 1.5, the decisive factor for the heat transfer, the thermal conductivity, decreases by a factor of up to 20 based on the transition from liquid to gas.

Moreover, another phenomenon which frequently occurs while using liquid nitrogen as a cooling medium is the Leidenfrost effect [5]. If the temperature of the surface to be cooled exceeds the so-called Leidenfrost temperature, an insulating gas layer between liquid and the solid surface is formed, which prevents any direct contact of the liquid and the solid [5, 6]. Based on the already mentioned adverse change of the thermal conductivity, the heat transfer and thus the cooling effect is significantly reduced [7].

2.2. LN_2 assisted machining of titanium alloys

Hong and Ding [1] compared dry, emulsion and LN_2 assisted turning of Ti-6Al-4V. The approaches were investigated experimentally and ordered by means of the occurring tool temperatures (highest to lowest): dry cutting, cryogenic tool back cooling, emulsion cooling, precooling the workpiece, cryogenic flank cooling, cryogenic rake cooling, and simultaneous rake and flank cooling. In the additionally conducted FEM simulations, reasonable thermal boundary conditions were applied: The heat transfer coefficient for cryogenic cooling increased with the tool surface temperature, being 23.72 kW/(m²K) at 93 K and 46.75 kW/(m²K) at 923 K. The paper demonstrates that the LN_2 application position has a major influence on the cooling effect, which can be calculated adequately by FEM simulations. However, neither the simulated mechanical loads were compared to experiments, nor the basic chip geometry.

Bermingham et al. [8] investigated the effectiveness of cryogenic cooling during turning of Ti-6Al-4V at constant cutting velocity. Cutting with rake and flank cooling was compared to dry cutting. The LN_2 application prolonged the tool life between 43% and 58%. Increasing the feed rate and in terms reducing the cutting thickness to maintain the same material removal rate, drastically reduced the tool life in both cases, dry and LN_2 cutting. This means that LN_2 cooling lowers the tool temperatures only to a certain extent.

Bordin et al. [9] investigated dry and LN_2 assisted turning of additively manufactured Ti-6Al-4V by experiments and FEM simulations. The cryogenic cooling was implemented at the flank face and the new surface of the workpiece with a heat transfer coefficient of 20 kW/(m²K) and a nitrogen temperature of 77 K. The material parameters and the friction coefficients were calibrated to meet the cutting forces for two experimental parameter sets. Thereby, the trends in the cutting forces and temperatures were predicted correctly.

Davoudinejad et al. [10] investigated dry and LN_2 assisted orthogonal cutting of Ti-6Al-4V by experiments and FEM simulation. The chip formation simulation with a cutting length of 2 mm was realized by the FEM Software Advantedge using the provided remeshing technique. Cryogenic cooling was implemented via the unrealistically high heat transfer coefficient 2000 kW/(m²K) in a radius of 1.5 mm at the rake face, where no further explanations are given.

Sun et al. [11] compared flood cooled, minimum quantity lubrication (MQL) and LN_2 assisted turning of Ti-5553 by experiments and FEM simulations. The temperature driven mechanisms adhesion and crater wear have been identified as crucial for the tool wear. Consequently, the cooling by LN_2 resulted in the lowest tool wear, followed by flood cooling and MQL. In the FEM Simulation cryogenic cooling was realized by a heat exchange window at the flank face with a transfer coefficient of 10000 kW/(m²K), which is even higher than in [10].

The literature review demonstrates, that LN_2 cooling efficiently lowers temperatures when machining titanium alloys and thereby reduces tool-workpiece adhesion and tool wear. This permits a tool life of several minutes. For such processes a stationary thermal tool state can be assumed, which in turn must be considered in numerical cutting simulations. For a sufficient LN_2 cooling in the simulation of orthogonal cutting, in some cases unphysically high heat transfer coefficients have been used. This may be attributed to the restricted cooling area, which is available in orthogonal cutting. In the following sections a model is presented to simulate orthogonal cutting with rake face or tool internal LN_2 application, which overcomes the before mentioned issues. In the first step, the modelling of the heat transfer coefficient of LN_2 cooling is explained.

3. Model

3.1. Heat transfer from surface to coolant

The finite element method is a commonly used technique to analyze machining operations [1, 9, 10, 11]. To simulate the cryogenic cooling in addition to the machining process, the behavior of the coolant fluid has to be modeled as well.

A widespread approach to describe the heat transfer rate for convection problems in an efficient way is

$$\dot{q} = h_{LN2}\,(T_{boil} - T_{surf}), \tag{1}$$

where the heat transfer coefficient h_{LN2} can be a function of various flow parameters [4]. Note that T_{boil} is the boiling temperature of the fluid (and therefore known) and T_{surf} is the iteratively determined surface temperature at the present node. Based on the relatively lower pressure fluctuations during the expansion of the fluid to the environment, T_{boil} is assumed as constant. If h_{LN2} is known, the resulting heat flux rate $\dot{q}$ can be calculated.

3.2. Implementation of cryogenic cooling in the simulation

The success of using Eq. (1) depends on an accurate determination of h_{LN2}. Up to now, only a small number of published works describing h_{LN2} for the cryogenic case can be found [4]. In addition, there are strong variations of h_{LN2} for different flow regimes and it shows a strong dependence on several flow parameters such as flow velocity, vapor content, angle of inflow (overflowing surface or impingement jet) or the surface temperature [4].

The values for h_{LN2}, which can be found in the literature differ among authors, but no uniform description for h_{LN2} is given [4]. In the case of an impinging jet, the heat transfer coefficient varies from 2 kW/(m²K) up to 74.95 kW/(m²K), whereby no potential dependency on the surface temperature T_{surf} is used [4]. Furthermore, detailed conditions of the flow field are not given in many studies.

A model, which describes the cryogenic heat transfer of LN_2 overflowing a hot surface, where the dependence on different flow parameters is taken into account, was developed [12].

Based on detailed simulations the heat transfer coefficient h_{LN2} can be determined. In Fig. 1 the resulting values for the interesting surface temperature range are given, which are of the same order of magnitude as typical literature values for the impinging jet.

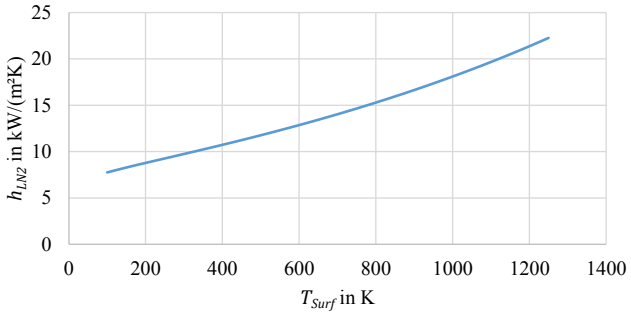

Fig. 1. Temperature depending heat transfer coefficient for the interesting flow velocity [12]

In addition, the detailed model makes it possible to adapt the flow parameters to the respective case in order to enable a determination of h_{LN2} for a various number of applications. However, to validate Eq. (1), a basic experiment (with a relatively easy geometry) was developed, which gives access to perform comprehensive measurements of the cooling behavior. Therefore, a specimen consisting of Ti-6Al-4V is heated up to the process-relevant temperature in order to subsequently cool it down with LN2 in an equivalent way sketched in Fig. 2. The heat transfer coefficient shown in Fig. 1 shows a good agreement with the experimental data.

3.3. Chip formation simulation

To simulate orthogonal cutting of Ti-6Al-4V the FEM Software Abaqus Standard 17.0 is used. The process parameters of the chip formation simulation were kept constant and are given in Table 1.

Table 1. Process parameters of the orthogonal cutting simulation.

parameter	v_c	h	l_c	α	γ	r_β	μ
unit	m/min	µm	µm	°	°	µm	-
value	100	100	500	7	0	40	0.2

Hereby v_c denotes the cutting velocity, h the cutting thickness, l_c the cutting length, α the clearance angle, γ the rake angle and r_β the cutting edge radius. Friction between tool and workpiece was considered using Coulomb's law. The coefficient of friction μ was kept constant for each simulation, because of the contradictory trends in the reviewed literature: Compared to dry conditions, μ decreased in [13], didn't change in [14] and slightly increased in [8] due to LN_2 application.

The simulation model used in this work is an adapted version of one presented in [15]. Assumed is a plane strain state with a model thickness of 1 µm. A basic feature of the model is a self-developed workpiece remeshing routine. Remeshing is performed by pre-/postprocessing scripts after each 5 µm of cutting length. For the simulation of cryogenic cutting, this calculation pause is also used to detect the surface edges, lengths and temperatures and to update the values of the resulting heat fluxes. Constitutive Material modeling is realized by v. Mises plasticity and a Johnson Cook flow stress equation with parameters according to [16]. Material fracture and the referring flow stress reduction is also modeled by a Johnson Cook approach using damage parameters according to [17]. The parameters are summarized in Table 2 and Table 3.

Table 2. Johnson Cook flow stress parameters for the cutting simulation. [16]

parameter	A	B	n	c	m	T_m	T_0
unit	MPa	MPa	-	-	-	K	K
value	724.7	683.1	0.47	0.035	1.0	1953	293

Table 3. Johnson Cook damage parameters for the cutting simulation. [17]

parameter	D_1	D_2	D_3	D_4	D_5
value	-0.09	0.25	-0.5	0.014	3.87

Zanger [15] used these parameters for dry orthogonal cutting with v_c = 100, 200 and 300 m/min and h = 100 µm. He showed that the simulated cutting forces generally suit the experimental values, partly exceeding them by less than 15%. This ensures a realistic cutting power in the simulation for both, dry and cryogenic cutting, as the (main) cutting forces hardly differ for both cooling concepts according to literature [8, 9] and own measurements in recent experiments. The values for v_c and l_c used in this work result in a simulated process time of 0.3 ms. However, the scope of this work is the simulation of thermo-mechanical loads, which occur in long-running cutting experiments. Hence the following is assumed for the thermal conditions: The chip is in a transient thermal state, which requires a detailed modelling of the specific heat capacity and the heat conductivity. Here the values determined by Milošević and Aleksić are used [18]. Unlike the chip, the tool is in a thermal steady state, in which the workpiece interaction and the applied boundary conditions define the tool temperature field. To reach the steady tool state within the cutting simulation time, the physical material parameters must be altered without manipulating the equilibrium temperatures or heat fluxes. A convenient method proposed by

Lorentzon and Järvstråt [19] is the reduction of the tool's specific heat capacity, which was validated by Zanger [15] and is also used here.

Two cryogenic cooling approaches are analyzed in this work, the rake face and the tool internal LN_2 application. The tool dimensions as well as the referring thermal boundary conditions are depicted in Fig. 2.

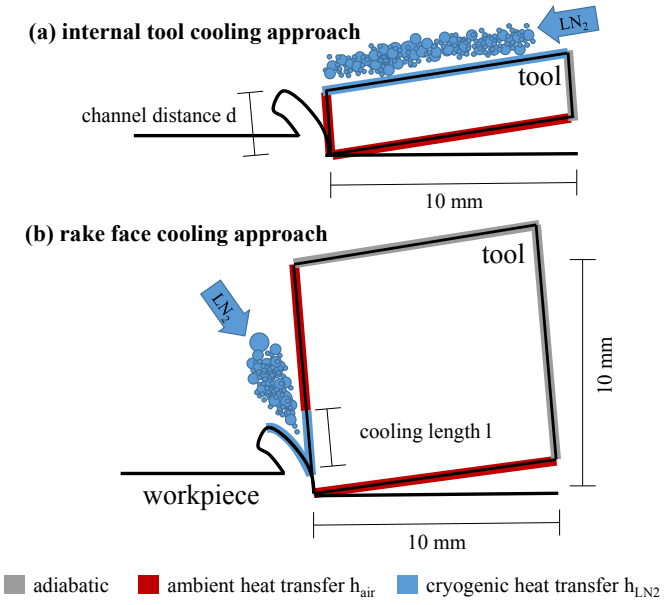

Fig. 2. Thermal boundary conditions for (a) Tool internal LN2 application, (b) Rake face LN2 application

The tool internal LN_2 application is modeled by a cryogenic heat transfer along the lower side of the cutting channel, which is depicted in Fig. 2 (a). To realize such a coolant supply, the cutting edge stability has to be traded off against the cooling efficiency. Based on that the channel distance d was varied. To evaluate the cooling effect and to identify a suitable position, the following channel distances are regarded in the chip formation simulation: 0.5 mm ("d=0.5") and 1.5 mm ("d=1.5"). It is essential to define reasonable boundary conditions for the entire model. At the red marked faces in Fig. 2 (a), a convective ambient heat transfer with an air temperature of T_{air} = 293 K and a heat coefficient of h_{air} = 100 W/m²K is assumed. Further it is assumed that the grey marked boundary is in direct contact with the tool holder resulting in a heat conduction from the insert to the tool holder. At the current time, the temperatures occurring in this zone are unknown. Upcoming investigations will determine the typical magnitude of the resulting temperatures to further improve the simulation's quality. By selecting an adiabatic boundary condition at the grey marked edges for the tool internal and the rake face LN_2 application, comparable conditions for the evaluation of the cooling effect are accomplished. Furthermore, the most conservative case is covered, i.e. the case in which the highest tool temperatures occur.

The rake face application is modeled by a cryogenic heat transfer not only at the tool face, but also at the chip in front of the rake face, which is illustrated in Fig. 2 (b). The highest point of contact between tool and chip is taken as the lower border of LN2 application. The highest point of the rising chip is taken as upper border for the cryogenic heat transfer.

In Fig. 3 the contour plot of the Abaqus variable *CFL11* is depicted, which is the concentrated heat flux in µW at the element boundary nodes. Consequently, a constant heat flux $\dot{q}$ at different elements may cause various values of *CFL11* depending on elements' edge lengths. Fig. 3 also gives an impression of the element sizes after remeshing. The typical edge length of elements in the chip is approx. 3 µm. The axes for the evaluation of the rake and flank face temperatures are depicted as well.

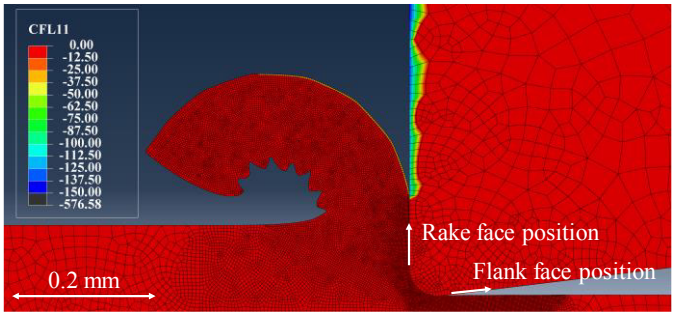

Fig. 3. Detailed heat fluxes in the rake face cooling simulation l=2.5

One goal of the simulation is to identify the effect of the cooling length l along the rake face on the tool temperatures. Therefore, the following cooling lengths were regarded in the simulation: 2.5 mm ("l=2.5") and 5.0 mm ("l=5.0"). A combination of internal and rake face LN_2 application with the channel distance 1.5 mm is also investigated ("d=l=1.5").

The cryogenic approaches will be compared to reference simulations, which represent orthogonal dry cutting with a heat transfer through the tool holder. The model dimensions equal those of the rake face cooling in Fig. 2 (b). But instead of cryogenic heat transfer, ambient conditions are modeled on the rake face. In the dry cutting simulation an adiabatic boundary at the tool internal (grey marked) interfaces of the model, similar to the cryogenic cutting simulation, would cause a tool heating up to the maximum chip temperature. To avoid such unphysical behavior, the simulation permits the definition of boundary temperatures, which cause a heat transfer out of the tool. The exact temperatures at the interface edges are unknown as already mentioned above. For the present work, the following temperatures were selected at the grey marked interfaces of Fig. 2 (b): 293 K ("T=293") and 473 K ("T=473"). The boundary temperature of 293 K represents the physical limit case of no edge heating. The boundary temperature of 473 K represents a significant heating of the tool interfaces, which have a distance of approx. 10 mm to the cutting zone. Table 4 outlines the varied boundary conditions of each simulation regarded in this work.

Table 4. Boundary condition overview.

Simulation	tool interface condition	channel distance d	cooling length l
T=293	T=293 K	-	0 mm
T=473	T=473 K	-	0 mm
d=0.5	adiabatic	0.5 mm	0 mm
d=1.5	adiabatic	1.5 mm	0 mm
d=l=1.5	adiabatic	1.5 mm	1.5 mm
l=2.5	adiabatic	-	2.5 mm
l=5.0	adiabatic	-	5.0 mm

4. Results and Discussion

To compare the cooling approaches, in Table 5 the extracted heat of the specific cooling mechanisms is given. The unit mW/µm reflects the model thickness. The ratio of cumulated extracted heat to the cutting power (“cooling ratio”) is given as well. The values were determined at the last simulation step.

Table 5. Heat extraction of specific cooling mechanisms.

	cutting power	tool cooling		wp/chip cooling	cooling ratio
		conductive	convective		
Simulation	mW/µm	mW/µm	mW/µm	mW/µm	%
T=293	398.36	19.59	0.37	0.07	5.03
T=473	398.71	10.82	0.88	0.07	2.95
d=0.5	401.34	0	20.66	0.07	5.17
d=1.5	403.20	0	22.47	0.07	5.59
d=l=1.5	404.92	0	29.94	4.78	8.57
l=2.5	398.98	0	24.1	4.86	7.26
l=5.0	398.59	0	27.87	4.76	8.19

The cooling approach does hardly influence the cutting power because of similar cutting forces. To explain this in the context of the simulation, it must be considered that the cooling approaches hardly affect the temperatures and thus the flow stress in the primary shear zone. Furthermore, the influence of the cryogenic cooling on the friction was not modeled.

In the dry cutting simulation T=293 the rate of heat extracted by conductive tool cooling is comparable to the rate extracted by cryogenic cooling in the simulation d=0.5. With the boundary temperature of 473 K the extracted heat nearly decreases by 50%. This indicates that conductive heat transfer may not be neglected and the selected boundary conditions at the tool interface must be known when simulations should be compared to experimental results. However, the convective heat transfer at the tool (“tool cooling”) and the workpiece/chip (“wp/chip cooling”) due to ambient conditions is insignificant.

For the comparison of the cryogenic approaches, the conductive heat transfer was disabled by selecting the boundary conditions as adiabatic at the referring interfaces. In the simulation of tool internal LN_2 application it is interesting to note that the smaller channel distance of 0.5 mm causes less heat extraction than the channel distance of 1.5 mm. This behavior can be explained by the tool temperature fields in Fig. 4 and the referring flank face temperature profiles in Fig. 6.

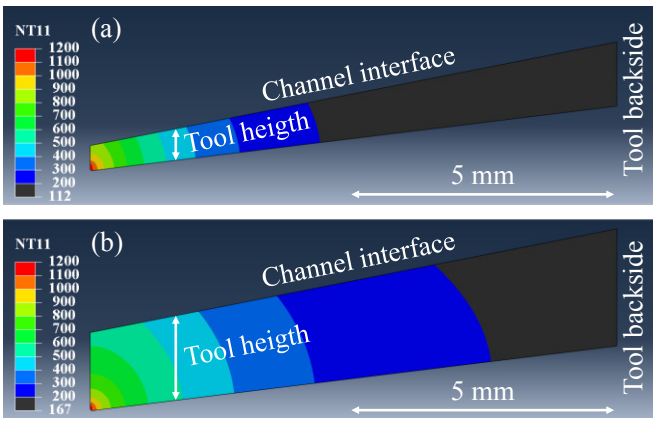

Fig. 4. Temperature field in K in the tool insert of the simulations (a) d=0.5 and (b) d=1.5

At the flank face position 840 µm the temperature in the simulation d=0.5 drops below the temperature in d=1.5, see Fig. 6. The temperature gap increases up to 55 K and remains up to the tool backside, see Fig. 4. Consequently, the rate of extracted heat over a major part of the channel edge in the simulation d=0.5 is smaller than in the simulation d=1.5. Within the smaller tool less heat is transported to the more distant parts of the channel edge, because the tool internal conduction from the cutting edge in direction of the tool backside occurs over a smaller tool height.

In addition to the channel cooling in the simulation d=1.5, the rake face and the chip is cooled as well in the simulation d=l=1.5. According to Table 5 this increases the total rate of extracted heat by more than 50%.

The results of the simulation l=2.5 in Table 5 demonstrate that locally concentrated rake face cooling efficiently extracts heat from the tool. Increasing the cooling length does improve the cooling effect. But the simulation l=5.0 indicates that this is only possible to a certain extent, as the rate of extracted heat increases by only 13% with a cooling length increase of 100% compared to the simulation l=2.5.

The cooling ratio range in Table 5 from 5.17 to 8.57 demonstrates that it is possible to significantly increase the extracted heat by appropriate LN_2 cooling and to exceed the rate of heat extracted by solid body conduction. The cooling ratio in the presented simulations is obviously limited to about 10% of the cutting power. The limit originates from the fact, that the major part of the heat is generated inside the workpiece material which makes a direct cooling impossible.

While the rate of extracted heat is of scientific interest, the resulting tool temperatures are relevant for the tool wear and thus the process costs. Therefore, the temperature profiles along the tool’s rake face and flank face are depicted in Fig. 5 and Fig. 6.

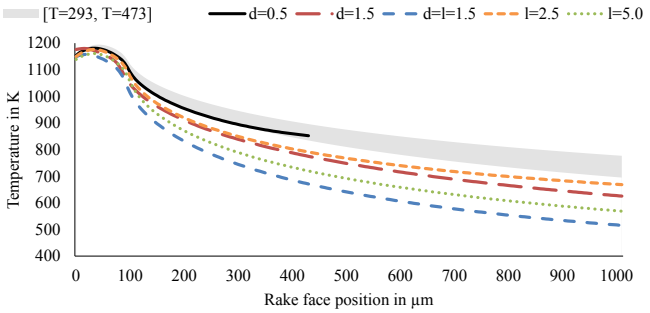

Fig. 5. Simulated rake face temperatures

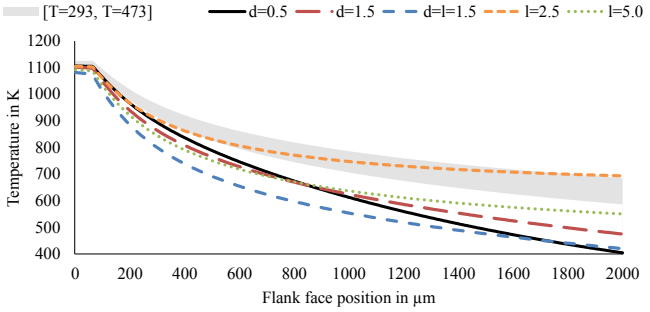

Fig. 6. Simulated flank face temperatures

The regarded intervals are chosen with respect to the high temperatures, which are critical in terms of tool wear. For reasons of clarity the tool temperatures of the dry cutting simulations are given as a grey marked intervals, whereas the upper boundary refers to simulation T=473 and the lower boundary to simulation T=293. The rake face temperatures of the simulation T=473 are clearly higher than those of the other simulations, while the rake face temperatures of the simulations T=293 and d=0.5 are on the same level.

Compared to the other cryogenic cooling simulations the rake face temperatures of the simulation d=0.5 are relatively high. This is counterintuitive but can be explained as follows: Cryogenic channel cooling directly only affects the highest node of the rake face. The resulting heat flux in this area is unable to reduce the temperatures at the entire rake face drastically. Cooling with the channel distance 0.5 mm rather effects the tool's flank face, where the lowest temperatures are observed at a certain distance from the cutting edge, see Fig. 6. Still, internal cooling with the channel distance 1.5 mm is more effective in reducing the critical tool temperatures close to the cutting edge.

The combination of tool internal and rake face cooling in the simulation d=l=1.5 generally results in the lowest temperatures in the wear relevant area close to the cutting edge.

Exclusively cooling the rake with a cooling length of 2.5 mm yields to rake face temperatures comparable to the simulation d=1.5, while the cooling length 5.0 mm causes even lower temperatures. Directly cooling the wear relevant tool sections is the most effective way to reduce the referring temperatures. Consequently, the flank face temperatures are less affected by rake face cooling. However, it must be noticed that the high flank temperatures at larger cutting edge distances are affected by the specified adiabatic tool boundaries.

5. Conclusion

In this work different cryogenic cooling approaches of orthogonal cutting of Ti-6Al-4V were compared among each other and to conductive tool cooling by means of FEM simulations. The main findings are:

- Cryogenic convective tool cooling with moderate heat transfer coefficients effectively extracts process heat and lowers tool temperatures, also compared to conductive tool cooling by prescribed boundary temperatures.
- The rate of extracted heat is restricted to values clearly below the process power, also in cryogenic cutting.
- Internal and external LN2 supply are promising process cooling alternatives in orthogonal cutting. In practical application it must be considered that external LN2 supply may be impaired by a tool chip contact length being longer than in the simulation.
- For the internal LN2 supply a distance between the channel edge and the flank face of 1.5 mm results in a better overall cooling and lower tool wear relevant rake and flank face temperatures than a distance of 0.5 mm. This indicates that it is possible to realize an effective internal tool cooling without deteriorating the cutting edge stability.

Acknowledgements

This work was funded by the DFG within the projects SCHU 1010/51-1 and MA 1205/24-1. The financial support is gratefully acknowledged.

References

[1] Hong SY, Ding Y. Cooling approaches and cutting temperatures in cryogenic machining of Ti-6Al-4V. International Journal of Machine Tools and Manufacture. 2001; 41(10):1417-1437.
[2] Jawahir IS, Attia H, Biermann D, Duflou J, Klocke F, Meyer D, Newman ST, Pusavec F, Putz M, Rech J, Schulze V. Cryogenic manufacturing processes. CIRP annals. 2016; 65(2):713-736.
[3] Barron RF, Nellis GF. Cryogenic Heat Transfer: Cryogenic Heat Transfer. CRC press; 2016.
[4] Pusavec F, Lu T, Courbon C, Rech J, Aljancic U, Kopac J, Jawahir IS. Analysis of the influence of nitrogen phase and surface heat transfer coefficient on cryogenic machining performance. Journal of Materials Processing Technology. 2016; 233:19-28.
[5] Chandra S, Aziz SD. Leidenfrost evaporation of liquid nitrogen droplets. Journal of heat transfer. 1994; 116(4):999-1006.
[6] Schroeder-Richter D. Ein analytischer Beitrag zur Anwendung der Thermodynamik irreversibler Prozesse auf Siedephänomene. Forschrittberichte VDI Reihe 3: Verfahrenstechnik Nr.251. VDI-Verlag; 1991.
[7] Ningegowda BM, Premachandran B. Numerical Simulation of Two-Dimensional Forced Convective Film Boiling Flow over a Horizontal Flat Surface. Procedia IUTAM. 2015; 15:256-263.
[8] Bermingham MJ, Kirsch J, Sun S, Palanisamy S, Dargusch MS. New observations on tool life, cutting forces and chip morphology in cryogenic machining Ti-6Al-4V. International Journal of Machine Tools and Manufacture 2011; 51(6):500-511.
[9] Bordin A, Imbrogno S, Rotella G, Bruschi S, Ghiotti A, Umbrello D. Finite element simulation of semi-finishing turning of electron beam melted Ti6Al4V under dry and cryogenic cooling. Procedia CIRP. 2015; 31:551-556.
[10] Davoudinejad A, Chiappini E, Tirelli S, Annoni M, Strano M. Finite element simulation and validation of chip formation and cutting forces in dry and cryogenic cutting of Ti–6Al–4V. Procedia manufacturing. 2015; 1:728-739.
[11] Sun Y, Huang B, Puleo DA, Jawahir IS. Enhanced machinability of Ti-5553 alloy from cryogenic machining: comparison with MQL and flood-cooled machining and modeling. Procedia CIRP. 2015; 31:477-482.
[12] Golda P, Schießl R, Maas U. Heat Transfer Simulation of a cryogenic cooling stream in machining operation, (submitted to International Journal of Heat and Mass Transfer).
[13] Hong, SY. Lubrication mechanisms of LN2 in ecological cryogenic machining. Machining science and technology. 2006; 10(1):133-155.
[14] Courbon C, Pusavec F, Dumont F, Rech J, Kopac J. Tribological behaviour of Ti6Al4V and Inconel718 under dry and cryogenic conditions - Application to the context of machining with carbide tools. Tribology International. 2013; 66, 72-82.
[15] Zanger F. Segmentspanbildung, Werkzeugverschleiß, Randschicht-zustand und Bauteileigenschaften: Numerische Analysen zur Optimierung des Zerspanungsprozesses am Beispiel von Ti-6Al-4V. PhD thesis, Karlsruhe Institue of Technology (KIT), 2012.
[16] Lee WS, Lin CF. Plastic deformation and fracture behaviour of Ti–6Al–4V alloy loaded with high strain rate under various temperatures. Materials Science and Engineering: A. 1998; 241(1-2):48-59.
[17] Sun J, Guo YB. Material flow stress and failure in multiscale machining titanium alloy Ti-6Al-4V. The International Journal of Advanced Manufacturing Technology. 2009; 41(7-8):651-659.
[18] Milošević N, Aleksić I. Thermophysical properties of solid phase Ti-6Al-4V alloy over a wide temperature range. International Journal of Materials Research. 2012; 103(6):707-714.
[19] Lorentzon J, Järvstråt N. Modelling tool wear in cemented-carbide machining alloy 718. International Journal of Machine Tools and Manufacture. 2008; 48(10):1072-1080.